Cancer Medicine Journal

Research Article | Vol 3 Issue S1

Effectiveness of Hypoxia-Induced Accumulation of Cancer Stem Cells in Head and Neck Squamous Cell Carcinoma

Bezerra MAS[1], Ferreira LAM[1], Kawasaki-Oyama RS[1], Nascimento MCA[1], Cuzziol CI[1], Castanhole-Nunes MMU[1], Pavarino EC[1], Maniglia JM[2] and Goloni-Bertollo EM[1*]

[1]Genetics and Molecular Biology Research Unit (UPGEM), Medical School of São José do Rio Preto (FAMERP), São José do Rio Preto, São Paulo, Brazil

[2]Department of Otolaryngology and Head and Neck Surgery, Medical School of São José do Rio Preto (FAMERP), São José do Rio Preto, São Paulo, Brazil

Correspondence should be addressed to Eny Maria Goloni-Bertollo, eny.goloni@famerp.br

Received Date: July 30, 2020; **Accepted Date:** August 25, 2020; **Published Date:** September 01, 2020

ABSTRACT

INTRODUCTION: The small number of cancer stem cells, which correspond to only 0.01% - 0.1% of total tumor cells, has been the biggest obstacle in understanding their biology and role in the origin and maintenance of tumors, their metastatic and recurrence potentials, and resistance to radio-chemotherapy. Therefore, promoting its accumulation will enable further studies and future advances in the diagnosis and treatment of head and neck cancer squamous cell carcinoma.

OBJECTIVE: To induce cancer stem cell accumulation in primary cell cultures of head and neck squamous cell carcinoma using a hypoxia chamber.

METHODS: Head and neck squamous cell carcinoma samples were cultured and subjected to hypoxia. Oxygen deprivation aimed to induce cancer stem cell accumulation.

RESULTS: Immediately after hypoxia, the percentage of O_2-deprived cancer stem cells increased 2-fold as compared to control. Surprisingly, new phenotyping performed 45 days after hypoxia showed a 9-fold increase in cancer stem cell percentage in cells that suffered hypoxia. Hypoxic cells showed an increase in spheroid formation when compared to control cells, as well as enhanced abilities in invasion and migration.

CONCLUSION: Hypoxia was efficient in cancer stem cell accumulation. As cancer stem cells are a small number of cells within the tumor, promoting their accumulation will enable further studies and future advances in the diagnosis and treatment of head and neck cancer.

KEYWORDS

Cancer stem cells; Hypoxia; Head and neck squamous cell carcinoma

Citation: Bezerra MAS, Effectiveness of Hypoxia-Induced Accumulation of Cancer Stem Cells in Head and Neck Squamous Cell Carcinoma. Cancer Med J 3(S1): 13-23.

INTRODUCTION

Oxygen (O_2) is an essential substrate for aerobic organisms to produce energy. In many physiological or pathological states, organisms are in hypoxia, which means there is insufficient O_2 availability. Hypoxia leads to the excessive accumulation of free radicals that cause damage to proteins and cellular DNA. Under these conditions, cells temporarily arrest the cell cycle, reduce energy consumption, and secrete survival and pro-angiogenic factors. These adaptive responses that cells activate in O_2 deprivation conditions are coordinated by several cellular pathways, including gene regulation by factors induced by hypoxia (HIF) [1].

Hypoxia is commonly seen in several types of cancers, and it is associated with greater tumor aggressiveness [2-4]. The hypoxic tumor microenvironment (TME) contributes to metastasis, treatment failure, and patient mortality [5-7]. Increased HIF expression promotes metastasis through metabolic reprogramming. Cell morphology is altered, which contributes to increased mobility and, thus, induces the epithelial-mesenchymal transition [6,8], a necessary process for metastasis and tumor progression [9]. In addition, low O_2 availability in TME is associated with evasion of the immune system, resistance to radio and chemotherapy, and maintenance of cancer stem cells (CSC) [10].

Known as tumor initiator cells, CSCs are a subpopulation of tumor cells that have properties similar to normal stem cells (SC) [11,12]. Increasing evidence indicates that hypoxia has a significant effect on the maintenance and evolution of CSCs, indicating that these cells are regulated by HIFs [12]. Therefore, in this study, we evaluated the hypoxia effects on CSC accumulation in head and neck squamous cell carcinoma (HNSCC).

MATERIAL AND METHODS

This study of human tumor samples was approved by the Human Research Ethics Committee at São José do Rio Preto School of Medicine (CEP/FAMERP CAAE 60735316.9.0000.5415). Resected surgical specimens were obtained from untreated patients with HNSCC [13] at Base Hospital, after obtaining informed consent.

Cancer Tissue Preparation and Culture

The samples were immediately transported to the lab in Dulbecco`s Modified Eagle's Medium (DMEM, Sigma) containing 2% antibiotic/antimycotic (AB/AM) (Gibco) at room temperature. The specimens were washed with phosphate-buffered saline, and necrotic tissue was removed with a scalpel. Then, the samples were minced with scissors and digested with DMEM containing 100 U/mL collagenase type I (Gibco) overnight at 37°C. The digested specimens were sequentially washed with DMEM. The cells were seeded into culture flasks with DMEM/HAM F-12, supplemented with 10% fetal bovine serum (FBS) (Gibco), 1% AB/AM, and 1% glutamine (Sigma) and was maintained at 37°C in a humidified 5% CO_2 incubator.

Figure 1: Items that compose the hypoxia chamber; 1: Clips used to seal; 2: Plastic bag; 3: O_2 absorbers; 4: Cell culture flask; 5: O_2 sensor.

Hypoxia Chamber

The cell culture was sealed inside a plastic bag with an O_2 absorber and an O_2 sensor. Upon reaching hypoxia, an O_2 concentration below 2%, a clip was used to separate the cells in cultivation from the O_2 absorber hermetically, thus keeping the O_2 concentration within the desired area stable [14] (Figure 1). All samples were submitted to hypoxia for 12 hours. As a control, the same samples were used in the normoxic condition, which is normal O_2 availability.

Phenotyping by Flow Cytometry

To evaluate CSC presence, all cultured cells, hypoxic and normoxic, were phenotype measuring aldehyde dehydrogenase 1 (ALDH1) activity (ALDEFLUOR Assay Buffer, STEMCELL Technologies) and CD44 (BD Biosciences) and CD133 (Thermo Fisher Scientific) positivity expression using flow cytometry FACSCalibur (BD), according to the manufacturer's protocols.

Tumorigenic Potential Evaluation

Tumor sphere formation assay

To generate spheroids, hypoxic and control cells were seeded on ultra-low attachment 6-well plates (Corning) at a density of 2.5×10^3 cells/well and grown for 5 days. Spheres were cultured in DMEM supplemented with 10% FBS and 1% AB/AM. Cells were maintained in a 5% CO_2-humidified incubator at 37°C. Every day, sphere formation was observed with minimal disturbance [15]. All tumorsphere assays were photographed on day 0 and day 5.

Tumor cell migration assay

For tumor cell migration assay, 2.5×10^3 hypoxic and control cells, suspended in 200 µL serum-free medium, were seeded over each trans-well chamber, containing a polycarbonate filter membrane (8 µm diameter pores), in 24-well plates (BD BioCoat migration chamber). DMEM supplemented with 10% FBS was placed in the lower chamber as a chemoattractant. Cells were incubated for 12 hours at 37°C in a 5% CO_2 humidified incubator. Invasive cells reaching the bottom of the filter membrane were fixed with 4% formaldehyde for 2 minutes and methanol for 20 minutes and then stained with 5% Giemsa. The number of migrated cells on each membrane was counted in 5 random fields at 100X magnification under an inverted microscope. Each experiment was repeated three times.

Tumor cell invasion assay

Hypoxic and normoxia cells were seeded over a matrigel invasion chamber in 24-well plates (BD BioCoat matrigel invasion chamber) at 2.5×10^3 cells/200 µL serum-free medium per well density. The lower chambers were filled with DMEM medium containing 10% FBS as a chemoattractive. After incubation for 12 hours at 37°C, cells migrating to the underside of the membrane were fixed with 4% formaldehyde for 2 minutes and methanol for 20 minutes, and stained with 5% Giemsa. The cells remaining on the upper surface of the membrane were removed with a cotton swab. The number of invaded cells on each membrane was counted in 5 random fields at 100X magnification under an inverted microscope. Each experiment was repeated three times.

Reverse transcription-quantitative polymerase chain reaction (RT-qPCR)

The RT-qPCR analysis was performed on StepOne plus (Applied Biosystems). Total RNA was extracted from hypoxic and normoxic cells using a Direct-Zol RNA MiniPrep plus Kit (Zymo Research), cDNA was synthesized using a high capacity cDNA reverse transcription kit (Thermo Fisher Scientific), and a TaqMan probe (PCR Master Mix - Life Technologies) was used for the PCR reaction. Amplification of two housekeeping genes, GAPDH (Thermo Fisher Scientific) and RPLPO (Thermo Fisher Scientific), were used as an internal standard. The comparative Ct method was applied

to determine the fold-change in expression levels relative to the control samples, according to the formula ΔΔCt ($2^{-\Delta\Delta Ct}$) [16].

Western blot analysis

Protein was sequentially extracted from the flow-through, obtained after RNA extraction in Zymo-Spin IICR Collum (Direct-Zol RNA MiniPrep plus Kit (Zymo Research)). The protein was quantified with a Pierce BCA Protein Assay Kit (Thermo Scientific) in a spectrophotometer. Total protein (16 µg) was run in Bolt 4 Bis-Tris to 12 Bis-Tris, 10 well, mini protein gel (Invitrogen), and transferred to an iBlot Transfer Stack polyvinylidene difluoride (PVDF) membrane using the iBlot Gel Transfer Device (Invitrogen). The PVDF membrane was blocked in 5% BSA/TBS-T 1× for 1 hour at room temperature, followed by the incubation with anti-HIF1α (Invitrogen) and anti-NANOG (Invitrogen) primary antibodies overnight at 4°C. Subsequently, the PVDF membrane was incubated with appropriated secondary antibodies conjugated to horseradish peroxidase (Sigma) for 1h at room temperature. The signal was developed using the ECL Western Blotting Substrate (Thermo Scientific), and blots were visualized by chemiluminescence. The relative amount of protein on the blots was determined by densitometry using an ImageJ program. β-actin was detected on the same membrane and used as a loading control (The relative expression of interesting protein = sample gray value/β-actin gray value).

Statistical analysis

Flow cytometry counting of ALDH+/CD44+/CD133+ populations was analyzed using FlowJo software (Tree Star, Ashland Ore) to establish final gating and positive phenotype proportions in each sample (Cell Quest Pro).

Statistical analysis was performed using Prism 6.01 (GraphPad Software). The statistical tests used were the D'Agostino and Pearson's normality test, a t-test for one sample, the Wilcoxon signed-rank test, and the Mann-Whitney test. Data were expressed as median and mean ± standard deviation. A value of $p < 0.05$ was considered statistically significant.

RESULTS

Sample Description

A total of 24 HNSCC samples were collected. Of these, 14 samples did not grow, or were contaminated. Among the remaining 10 samples, 50% was lost due to contamination or senescence, and a final sample size of 5 was used in this study (Table 1). Most patients were men (95.8%) with a history of smoking (87.5%) or alcoholism (58.3%), with an average age of 63.25 years (+/-8.61 standard deviation) (range 49-80). Only 11 patients (45.8%) were tested for p16, of which 27.3% were positive while 72.7% were negative. Regarding the anatomical site, 37.5% of samples came from larynx, 33.3% oral cavity, 20.8% oropharynx, and 8.3% nasopharynx and hypopharynx. The demographic and clinical pathological characteristics of patients are shown in Table 1.

Hypoxia Leads to ALDH1 +/CD44 +/CD133+ Cells Accumulation

The ALDH1, CD44, and CD133 markers were used to assess the presence of CSCs. Immediately after hypoxia, the percentage of CSCs increased 2-fold in cells that suffered O_2 deprivation as compared to control. The median for CSCs was 1.49% in cultures submitted to the hypoxia chamber, while the median for the control was 0.69%. Surprisingly, new phenotyping performed 45 days after hypoxia showed a 9-fold increase in the CSC percentage in cells that suffered hypoxia. The median of cells with triple-positive staining was 2.10% and 0.23% in the cells that passed through the hypoxia chamber and in control cells, respectively. Figure 2 describes the comparison of the percentage of CSCs between primary

cultures subjected to hypoxia and their respective controls immediately after hypoxia and 45 days after.

Sample	Age	Gender	Anatomical Site	TNM classification	Smocking status[a]	Alcohol habit[a]	p16
HNSCC-1	59	M	Oropharynx	T4N1M0	smoker	alcoholic	+
HNSCC-2	70	M	Oral Cavity	T4N2M0	smoker	non-alcoholic	unknown
HNSCC-3	54	M	Oropharynx	T1N0M0	smoker	alcoholic	-
HNSCC-4	63	M	Larynx	T3N1M0	smoker	non-alcoholic	-
HNSCC-5	62	M	Oropharynx	T4N1M0	smoker	alcoholic	unknown
HNSCC-6	71	M	Larynx	T1N0M0	smoker	non-alcoholic	unknown
HNSCC-7	54	M	Oropharynx	T4N0M0	smoker	alcoholic	unknown
HNSCC-8	67	M	Nasopharynx	T3N3M1	smoker	non-alcoholic	-
HNSCC-9	57	M	Oral Cavity	T3N0M0	smoker	alcoholic	unknown
HNSCC-10	68	M	Oral Cavity	T2N0M0	smoker	non-alcoholic	-
HNSCC-11	67	M	Oral Cavity	T2N0M0	smoker	non-alcoholic	-
HNSCC-12	49	M	Larynx	T1N0M0	smoker	alcoholic	unknown
HNSCC-13	55	M	Oral Cavity	T4N0M0	smoker	alcoholic	unknown
HNSCC-14	58	M	Larynx	T3N0M0	smoker	alcoholic	+
HNSCC-15	50	M	Oral Cavity	T4N3M0	non-smoker	non-alcoholic	-
HNSCC-16	49	F	Oral Cavity	T2N1MX	non-smoker	non-alcoholic	+
HNSCC-17	70	M	Larynx	T4N0M0	smoker	alcoholic	-
HNSCC-18	67	M	Larynx	unknown	smoker	alcoholic	-
HNSCC-19	78	M	Larynx	T2N0M0	smoker	non-alcoholic	unknown
HNSCC-20	67	M	Hypopharynx	T2N1M0	smoker	alcoholic	unknown
HNSCC-21	80	M	Oral Cavity	T2N0M0	non-smoker	non-alcoholic	unknown
HNSCC-22	69	M	Larynx	T3N0M0	smoker	alcoholic	unknown
HNSCC-23	69	M	Oropharynx	T3N2M0	smoker	alcoholic	unknown
HNSCC-24	65	M	Larynx	T1N0M0	smoker	alcoholic	unknown

Table 1: Demographic and clinicopathology characteristics of HNSCC patients' samples.
Note: [a]: Data obtained from medical records.

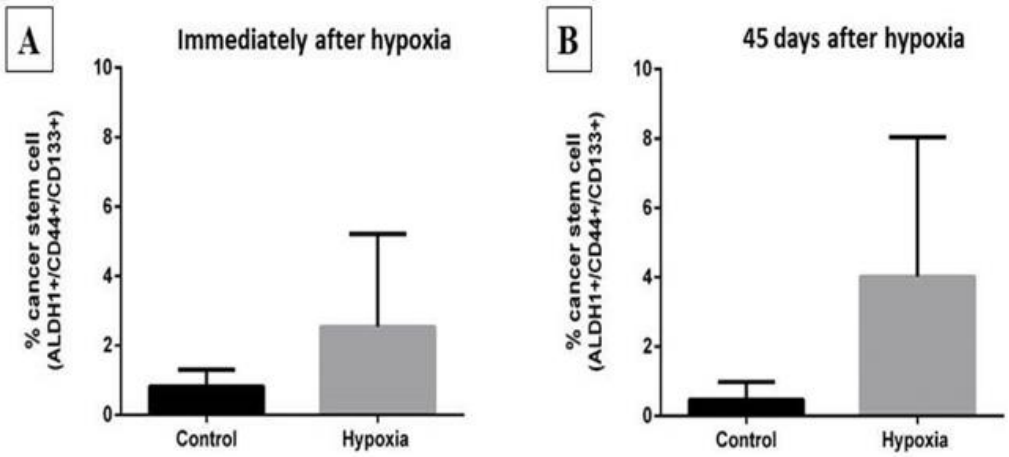

Figure 2: Cancer stem cell percentage between cells submitted to the hypoxia chamber and their respective controls. A) Phenotyping performed immediately after O_2 deprivation. B) Phenotyping performed 45 days after the cultures were submitted to hypoxia.

Hypoxia Leads to an Increased Tumorigenic Potential

Flow cytometry phenotyping showed that CSC accumulation was more evident 45 days after hypoxia. Thus, all trials that assessed CSC tumorigenic potential were performed 45 days after samples had passed through the hypoxia chamber.

All samples, hypoxia and control, were examined for spheroid forming capacity in ultra-low attachment plates. The CSC formed spheroids within 5 days. Hypoxic cells showed an increase in spheroid formation when compared to control cells. Representative images (Figure 3A). Cells that underwent O_2 deprivation formed a greater number of spheroids. These spheres were also larger and more compact in cells that suffered hypoxia. Invasion and migration were enhanced in all hypoxic cells, and p values were significant for each sample (Figure 3B & Figure 3C). The data show that hypoxia leads to an increase in the tumorigenic potential of HNSCC-derived cells.

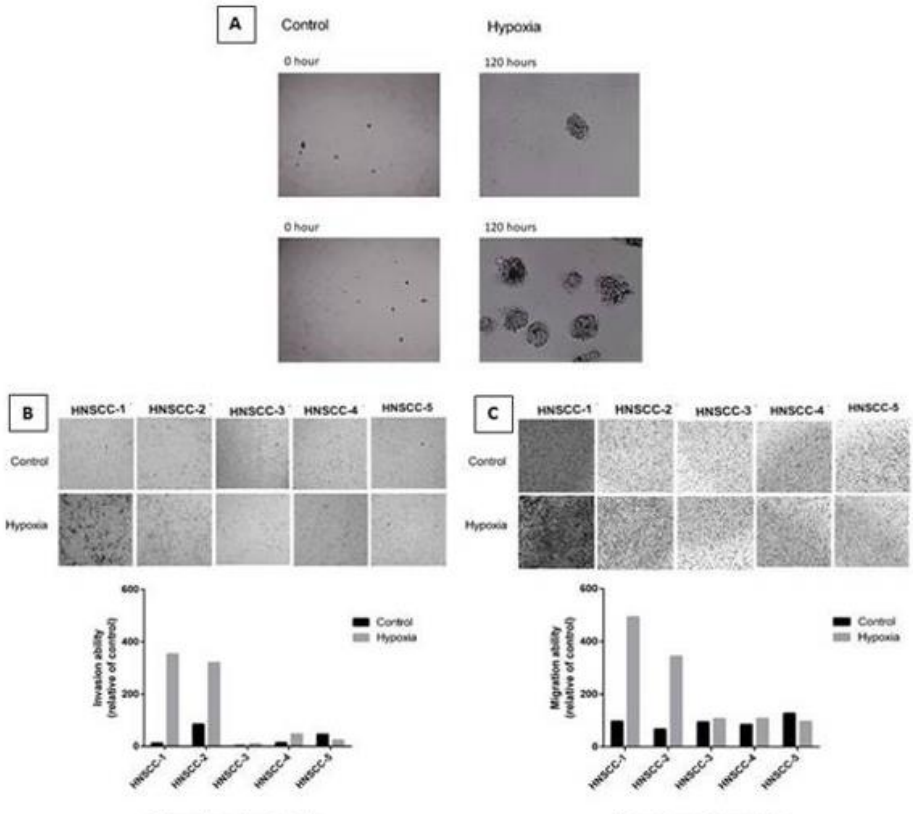

D

Mean values of invaded cells

Sample		mean	p
HNSCC-1	control	12.5	0,0078
	hypoxia	352.4	
HNSCC-2	control	84.5	0,0078
	hypoxia	319.6	
HNSCC-3	control	2	0,03
	hypoxia	9.6	
HNSCC-4	control	13.4	0,0015
	hypoxia	46.6	
HNSCC-5	control	45.9	0,0015
	hypoxia	24.1	

E

Mean values of migrated cells

Sample		mean	p
HNSCC-1	control	96.4	0,0005
	hypoxia	492.1	
HNSCC-2	control	67.4	0,0005
	hypoxia	342.8	
HNSCC-3	control	93.8	0,0005
	hypoxia	106.8	
HNSCC-4	control	84.8	0,0128
	hypoxia	107.2	
HNSCC-5	control	126.1	0,0002
	hypoxia	96.2	

Figure 3: Tests for tumorigenic potential. A) Tumorsphere formation assay. Representative images of HNSCC-3 primary culture. A larger number of spheroids formed in the sample submitted to hypoxia when compared to control. 40X magnification. B and C) 45 days after hypoxia, cells were subjected to tumor invasion and migration assays, respectively. Photomicrographs of the invaded and migrated cells (upper panels). 100X magnification. Cell counting of migrated and invaded cells from 5 separate fields (graphics below). D and E) mean values of the invasion and migration.

NANOG and HIF1A Gene and Protein Expression in Hypoxic HNSCC Cells

Gene expression analysis in primary cultures did not show any statistically significant difference between hypoxia and normoxia groups for *HIF1A* and *NANOG* with the median relative expression of 0.40 and 2.0, respectively (Figure 4A).

Relative quantification of protein expression showed no significant difference for HIF1A and NANOG proteins between hypoxia and normoxia groups. Median relative expressions for HIF1A and NANOG proteins in the control group were 1.3 and 0.03 and 1.4 and 0.4 in the hypoxia group, respectively (Figure 4B - Figure 4D).

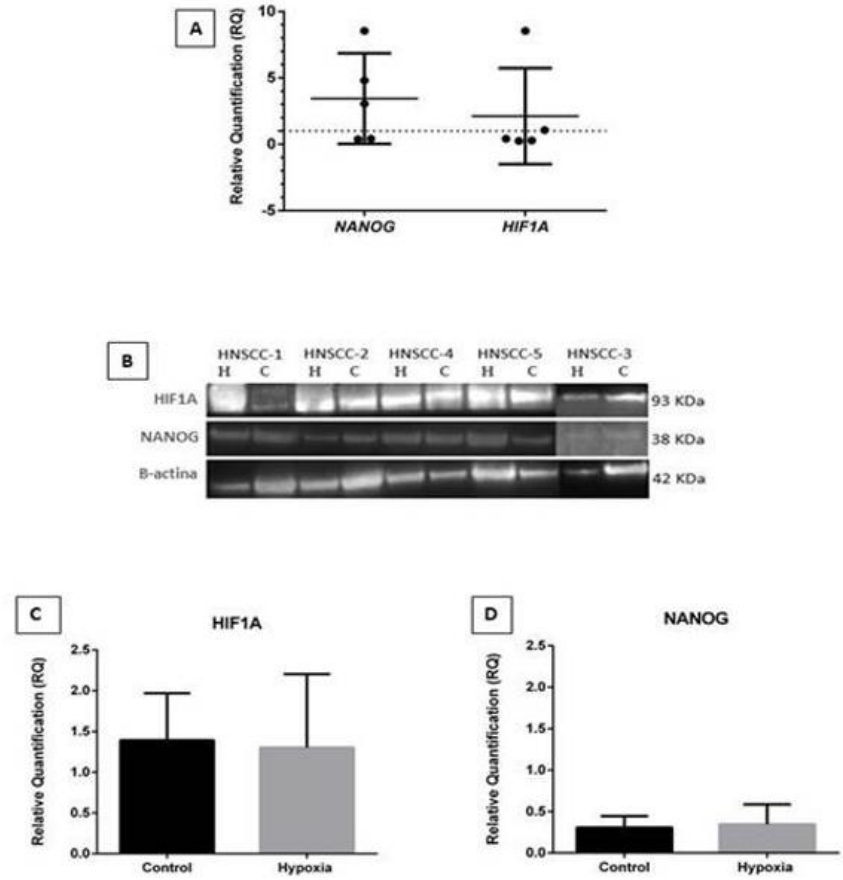

Figure 4: NANOG and HIF1A gene and protein expression. A) HIF1A and NANOG gene expression in primary cultures (RQ values in median). B) Western blot membrane photography. HIF1A, NANOG, and B-actin (endogenous) proteins. (H) Hypoxia (C) Control. C and D) RQ values from HIF1A and NANOG protein expression.

DISCUSSION

Head and neck cancer is the third most common cancer in the world. This tumor has a yearly incidence of 975,150 new cases with 46.42% mortality [17]. HNSCC is the most frequent head and neck cancer, representing 90% of cases. It originates in epithelial cells of the mucosal linings of the oral cavity, oropharynx, larynx, or hypopharynx [18,19].

The main risk factors for HNSCC are gender, age, and environmental factors such as smoking and excessive alcohol use [20,21]. Currently, the high-risk human

papillomavirus (HPV) infection, especially HPV-16 and HPV-18, has emerged as a risk factor for HNSCC, particularly in oropharyngeal tumors [18,22]. The p16 immunohistochemistry is commonly used as a surrogate marker for HPV detection in HNSCC, particularly for patients with oropharyngeal HNSCC [23]. For HNSCC, the HPV-positive status is a favorable prognostic marker, and it can be used for patient stratification [24,25].

In this study, most of the collected samples came from male patients with a mean age of 63.25 years and a history of alcoholism and smoking. The most affected anatomical regions were the larynx and oral cavity, followed by the oropharynx. Approximately 46% of patients were tested for HPV-16, of which 27% tested positive and 73% negative. One of the five samples analyzed was p16-positive. It was located in the oropharynx, T4N1M0 staging, and it had a greater capacity for invasion and migration in the analyses performed.

Despite the therapeutic advances made in recent years, HNSCC has a low survival rate, around 30% in five years [26]. This is partly due to the anatomical complexity of the region in which the cancer develops. In addition, HNSCC has different etiologies and a wide variety of molecular changes that lead to tumorigenesis. All of these factors result in a very heterogeneous cancer [18] making the HNSCC diagnosis often only possible in advanced stages of the disease.

Several cell types are part of TME, such as endothelial cells, fibroblasts, immune cells, among others. In addition, extracellular components, such as cytokines, growth factors, hormones, and extracellular matrix, surround tumor cells. The entire microenvironment is nourished by a vascular network [27]. TME cells produce factors that promote the self-renew ability of CSCs, stimulate angiogenesis, and recruit stromal cells, such as cells of the immune system, that secrete factors that induce cell invasion and metastasis [28]. Thus, TME not only plays a very important role in tumor initiation, progression, and metastasis, but it also affects the effectiveness of anti-tumor treatments [27].

Hypoxia plays a crucial role in TME, contributing to the development of the CSC phenotype, thus increasing the tumorigenic potential [28]. The reduction of O_2 availability causes changes in the TME pH, making it acidic, causing an imbalance between tumor cell proliferation and angiogenesis [14,29]. The acidic microenvironment around the cells also promotes protease activation that contributes to metastasis. In addition, abnormal angiogenesis limits chemotherapeutic drug delivery to cells resulting in resistance to treatment [28].

CSCs are presumed to originate from normal adult SCs or differentiated cancer cells, and they have a similar capacity to self-renew normal SCs [30]. CSCs correspond 0.01% to 0.1% of tumor cells, and they have surface markers similar to normal SCs, such as CD44 and CD133, as well as high intracellular expression of ALDH1. The high expression of ALDH1 is associated with an aggressive phenotype, resistance to treatment, and worsening clinical outcomes in various types of cancer [31]. Our results suggest that hypoxia contributes to CSC accumulation evidenced by higher levels of markers CD44+, CD133+, and ALDH1+ (Figure 2). Hypoxia also increased the invasive and migratory potential and tumorsphere formation in cells derived from primary HNSCC cultures (Figure 3).

NANOG is an important transcription factor that confers the potential for self-renewal to embryonic cells and induced pluripotent stem cells. Together with the transcription factors OCT4, SOX2, and KLF4, NANOG regulates pluripotency and the fate of embryonic SCs. Activation of transcriptional factors such as NANOG is

believed to enable cells to develop properties similar to SCs, acquiring differentiation and self-renewal capabilities [32]. Studies show that NANOG acts as an essential factor related to cell proliferation, cell invasion, and resistance to treatment [32,33]. The expression of this gene in precancerous lesions indicates that it can be a possible diagnostic marker. High expression of NANOG is associated with more advanced stages of the disease [33].

In our study, we observed a high expression of NANOG, and except for one sample (HNSCC-03), all the others showed high aggressiveness with tumor extension (T3 and T4) and involvement of regional lymph nodes (N1 and N2). The role of NANOG in cancer is not fully understood yet. It does not seem to act as a classic oncogene. Studies in transgenic mice have shown that overexpression of NANOG only induced the development of moderate hyperplasia in intestinal and stomach epithelium. However, when co-expressed with Wnt-1, NANOG increased the tumorigenic and metastatic capacity of breast tissue. These results show that NANOG appears to act as a cooperating or enhancing protumorigenic molecule [32].

The O_2 availability below the physiological demand in tissues leads to an adaptive response to hypoxia. HIFs are the primary regulators of O_2 homeostasis that control angiogenesis during hypoxia [34]. A recent HNSCC study demonstrated an increase in HIF1A expression in hypoxia conditions compared to normoxia in a model of salivary carcinoma. The increase in HI1A expression was associated with the aggressiveness of this tumor type [35]. Another study with normal and cancerous thyroid cell lines suggested differing regulation for HIFA subunits. HIF1A would be associated with the acute phase response to hypoxia and HIF2A with the chronic phase. The researchers observed that hypoxia induction increased the CSC population in the thyroid carcinoma cell line, suggesting that only the HIF2A subunit is associated with the phenotype of these cells, as it appears later [36].

Our results did not show a statistically significant difference in the gene and protein expression of HIF1A between HNSCC cells submitted to hypoxia and normoxia after 45 days of culture. Only one sample (HNSCC-05) showed overexpression of HIF1A. Possibly such results were observed because the analysis was performed a long time after hypoxia. We recognize that it is necessary to carry out an earlier analysis of gene and protein expression, as well as to evaluate the expression of the HIF2A subunit.

CONCLUSION

Our results demonstrated that hypoxia induces the accumulation of CSCs, evidenced by the high rates of CD44+/CD133+/ALDH1+ cells, as well as in the increase of invasiveness, migration, and tumorsphere formation potential observed in cells submitted to hypoxia.

The reduced CSC number within the tumor has been the biggest obstacle to understanding its biology and its role in the origin and maintenance of tumors. Therefore, promoting CSC accumulation will enable further studies and future advances in the diagnosis and treatment of head and neck cancer.

DATA AVAILABILITY

The data is maintained in the Genetics and Molecular Biology Research Unit - UPGEM, Medical School of São José do Rio Preto, FAMERP.

CONFLICTS OF INTEREST

There is no conflict of interest.

FUNDING STATEMENT

This work was supported by the Institution - The São Paulo Research Foundation (FAPESP) [grant number 2016/20087-1]; [grant number 2018/26166-6] and the

National Council of Technological and Scientific Development (CNPq) [grant number 310987/2018-0] and the Coordination for the Improvement of Higher Education Personnel - Brazil (CAPES) - Finance Code 001. Support by Medical School of São José do Rio Preto-FAMERP/Regional Faculty of Medicine of São José do Rio Preto FUNFARME.

ACKNOWLEDGEMENT

The authors are grateful the support by Medical School of São José do Rio Preto-(FAMERP)/Regional Medical School of São José do Rio Preto (FUNFARME), Base Hospital, Department of Otolaryngology and Head and Neck Surgery, especially Dr Luiz Sérgio Raposo, the contribution of Dr Carlos Viesi do Nascimento Filho for all help with the hypoxia chamber.

REFERENCES

1. Majmundar AJ, Wong WJ, Simon MC (2010) Hypoxia-inducible factors and the response to hypoxic stress. Molecular Cell 40(2): 294-309.
2. Graham K, Unger E (2018) Overcoming tumor hypoxia as a barrier to radiotherapy, chemotherapy and immunotherapy in cancer treatment. International Journal of Nanomedicine 13: 6049-6058.
3. Wigerup C, Påhlman S, Bexell D (2016) Therapeutic targeting of hypoxia and hypoxia-inducible factors in cancer. Pharmacology & Therapeutics 164: 152-169.
4. Jin Y, Wang H, Ma X, et al. (2015) Clinicopathological characteristics of gynecological cancer associated with hypoxia-inducible factor 1α expression: A meta-analysis including 6,612 subjects. PloS One 10(5): e0127229.
5. Semenza GL (2016) The hypoxic tumor microenvironment: A driving force for breast cancer progression. Biochimica et Biophysica Acta (BBA) - Molecular Cell Research 1863(3): 382-391.
6. Rankin EB, Nam JM, Giaccia AJ (2016) Hypoxia: Signaling the metastatic cascade. Trends in Cancer 2(6): 295-304.
7. Harper K, Lavoie RR, Charbonneau M, et al. (2018) The hypoxic tumor Microenvironment promotes invadopodia formation and metastasis through LPA1 receptor and EGFR cooperation. Molecular Cancer Research 16(10): 1601-1613.
8. Papale M, Buccarelli M, Mollinari C, et al. (2020) Hypoxia, inflammation and necrosis as determinants of glioblastoma cancer stem cells progression. International Journal of Molecular Sciences 21(8): 2660.
9. Markopoulos GS, Roupakia E, Marcu KB, et al. (2019) Epigenetic regulation of inflammatory cytokine-induced epithelial-to-mesenchymal cell transition and cancer stem cell generation. Cells 8(10): 1143.
10. Batlle E, Clevers H (2017) Cancer stem cells revisited. Nature Medicine 23(10): 1124-1134.
11. Abbaszadegan MR, Bagheri V, Razavi MS, et al. (2017) Isolation, identification, and characterization of cancer stem cells: A review. Journal of Cellular Physiology 232(8): 2008-2018.
12. Tong WW, Tong GH, Liu Y (2018) Cancer stem cells and hypoxia-inducible factors. International Journal of Oncology 53(2): 469-476.
13. Huang SH, O'Sullivan B (2017) Overview of the 8th edition TNM classification for head and neck cancer. Current Treatment Options in Oncology 18(7): 1-13.
14. Nascimento-Filho CH, Webber LP, Borgato GB, et al. (2019) Hypoxic niches are endowed with a protumorigenic mechanism that supersedes the protective function of PTEN. The FASEB Journal 33(12): 13435-13449.
15. Almeida LO, Guimarães DM, Squarize CH, et al. (2016) Profiling the behavior of distinct populations of head and neck cancer stem cells. Cancers 8(1): 7.
16. Livak KJ, Schmittgen TD (2001) Analysis of relative gene expression data using real-time quantitative PCR and the 2- ΔΔCT method. Methods 25(4): 402-408.

17. (2020) GLOBOCAN. Cancer tomorrow.
18. Leemans CR, Snijders PJ, Brakenhoff RH (2018) The molecular landscape of head and neck cancer. Nature Reviews Cancer 18(5): 269-282.
19. Gupta B, Johnson NW, Kumar N (2016) Global epidemiology of head and neck cancers: A continuing challenge. Oncology 91(1): 13-23.
20. Solomon B, Young RJ, Rischin D (2018) Head and neck squamous cell carcinoma: Genomics and emerging biomarkers for immunomodulatory cancer treatments. In Seminars in Cancer Biology 52(Pt 2): 228-240.
21. Cohen N, Fedewa S, Chen AY (2018) Epidemiology and demographics of the head and neck cancer population. Oral and Maxillofacial Surgery Clinics 30(4): 381-395.
22. Yete S, D'Souza W, Saranath D (2018) High-risk human papillomavirus in oral cancer: Clinical implications. Oncology 94(3): 133-141.
23. Bonner JA, Mesia R, Giralt J, et al. (2017) p16, HPV, and cetuximab: What is the evidence?. The Oncologist 22(7): 811-822.
24. Lechner M, Chakravarthy AR, Walter V, et al. (2018) Frequent HPV-independent p16/INK4A overexpression in head and neck cancer. Oral Oncology 83: 32-37.
25. Bhatia A, Burtness B (2015) Human papillomavirus-associated oropharyngeal cancer: Defining risk groups and clinical trials. Journal of Clinical Oncology 33(29): 3243-3250.
26. Gilormini M, Wozny AS, Battiston-Montagne P, et al. (2016) Isolation and characterization of a head and neck squamous cell carcinoma subpopulation having stem cell characteristics. Journal of Visualized Experiments 111: e53958.
27. Wu T, Dai Y (2017) Tumor microenvironment and therapeutic response. Cancer Letters 387: 61-68.
28. Carnero A, Lleonart M (2016) The hypoxic microenvironment: A determinant of cancer stem cell evolution. Inside the Cell 1(2): 96-105.
29. Melzer C, von der Ohe J, Lehnert H, et al. (2017) Cancer stem cell niche models and contribution by mesenchymal stroma/stem cells. Molecular Cancer 16(1): 1-15.
30. Peiris-Pagès M, Martinez-Outschoorn UE, Pestell RG, et al. (2016) Cancer stem cell metabolism. Breast Cancer Research 18(1): 1-10.
31. Ajani JA, Song S, Hochster HS, et al. (2015) Cancer stem cells: The promise and the potential. In Seminars in Oncology 42: S3-S17.
32. Jeter CR, Yang T, Wang J, et al. (2015) Concise review: NANOG in cancer stem cells and tumor development: An update and outstanding questions. Stem Cells 33(8): 2381-2390.
33. Grubelnik G, Boštjančič E, Pavlič A, et al. (2020) NANOG expression in human development and cancerogenesis. Experimental Biology and Medicine 245(5): 456-464.
34. Serocki M, Bartoszewska S, Janaszak-Jasiecka A, et al. (2018) miRNAs regulate the HIF switch during hypoxia: A novel therapeutic target. Angiogenesis 21(2): 183-202.
35. Wang HF, Wang SS, Zheng M, et al. (2019) Hypoxia promotes vasculogenic mimicry formation by vascular endothelial growth factor A mediating epithelial-mesenchymal transition in salivary adenoid cystic carcinoma. Cell Proliferation 52(3): e12600.
36. Mahkamova K, Latar N, Aspinall S, et al. (2018) Hypoxia increases thyroid cancer stem cell-enriched side population. World Journal of Surgery 42(2): 350-357.